

Entanglement of a two–qutrit Heisenberg XXZ model with Herring–Flicker coupling and Dzyaloshinskii–Moriya interaction in homogeneous magnetic field

Brahim Adnane^a, Younes Moqine^b, Abdelhadi Belouad^c, and Rachid Houça^{*a,c}

^a*LPMC. Laboratory, Theoretical Physics Group, Faculty of Sciences, Chouaib Doukkali University, PO Box 20, 24000 El Jadida, Morocco*

^b*Research Laboratory of Physics and Engineers Sciences, Team of Applied Physics and New Technologies, Polydisciplinary Faculty (FP-BM), Sultan Moulay Slimane University, Béni Mellal, Morocco*

^c*LPTHE. Laboratory, Theoretical Physics and High Energy, Faculty of Sciences, Ibn Zohr University, PO Box 8106, Agadir, Morocco*

Abstract

In this study, we use the concept of negativity to characterize the entanglement of a two–qutrit Heisenberg XXZ model for subject to a uniform magnetic field and z–axis Dzyaloshinskii–Moriya (DM) interaction with Herring–Flicker (HF) coupling. By varying the temperature, magnetic field, DM interaction, and distance of HF coupling. We find that the state system becomes less entangled at high temperatures or in strong magnetic fields, and vice versa. Our findings also suggest that entanglement rises when the z–axis DM interaction increases. Finally, HF coupling affects the degree of entanglement. For example, when HF coupling and temperature are at small values, the degree of entanglement is at its highest, but when HF coupling is at substantial values, the degree of intricacy tends to stabilize.

PACS numbers: 03.65.Ud, 03.67-a, 75.10Jm

Keywords: Two–qutrit, quantum entanglement, negativity, Heisenberg model, Herring–Flicker coupling, Dzyaloshinskii–Moriya interaction, density matrix.

*r.houca@uiz.ac.ma

1 Introduction

Entanglement is one of the most intriguing aspects of quantum physics [1]. It happens when particles interact in a manner that makes it impossible to characterize each particle's quantum state separately. With implementations in quantum communication and teleportation [2–4], quantum information processing [5], quantum dense coding, and the application of various quantum protocols [6–8], quantum entanglement uses are a precious resource for research that cannot be done using conventional resources. Different physics fields have also successfully attained entanglement. For instance, quantum logic operations involving trapped ions [10], nuclear spins of organic molecules [11], semiconductor devices [12], and atomic chips [13] have all been demonstrated to exhibit quantum communication patterns.

Finding a way to tell if a specific quantum system state is entangled or not, as well as selecting the optimal way to quantify the degree of entanglement, are significant challenges. In light of this, one of the most critical issues in the realm of quantum information is the quantization and characterization of the degree of entanglement. When the quantum system is in a pure state, the notion of entanglement is simpler and easier to comprehend. In contrast, the characterization of complete entanglement characteristics of mixed states is a challenging and unanswered mathematical problem. Several measures, such as negativity [14–17], have been suggested to quantify entanglement.

Condensed matter systems' quantum entanglement is a significant field, as is well known. Various studies on quantum entanglement have been accomplished on the thermal equilibrium states of spin chains subjected to an external magnetic field at a fixed temperature [18–22]. Moreover, two-qubit quantum correlations with the DM interaction receive much attention from researchers [23–27]. In addition, the Heisenberg model was used to study entanglement. A number of important works were produced, including the isotropic Heisenberg XX model [28,29], the XXX model [30–32], the anisotropic Heisenberg XY model [33,34], the completely anisotropic Heisenberg XYZ model [35], as well as some new research on the spin-1/2 [36]. Unfortunately, since measurements for higher spin systems are lacking, entanglement in spin-1 systems has gotten less attention. Vidal and Werner established a measure of entanglement called negativity, which may apply to higher spin systems [37,38]. Using the notion of negative, Wang et al. arrived at analytical conclusions about entanglement in a spin-1 chain [41,42].

Now, we describe a few studies by various authors that include the coupling strength, J , as a function of location in various spin chain configurations. In reality, due to quantum fluctuations and noise, the coupling intensity in quantum systems may be regarded as a factor in practical scenarios regarding the distance separating quantum particles. This method could be utilized to improve quantum implementations. In 1988 Haldane and Shastry [43,44] presented the first effort to explore entanglement in the spin chain with long-range interactions, where the coupling strength is equal to the inverse of the distance square and follows the squared law. In a similar manner, B. Lin et al. [45] investigated the XXZ Heisenberg chain with long-range interactions, whereas M. XiaoSan et al. [46] investigated the XX Heisenberg model with Calogero Moser interactions.

Due to the significance of HF coupling in quantum information physics to determine the degree of intricacy between particles and motivated by previous works, we will investigate

the thermal entanglement of spin-1 in a two-spin Heisenberg XXZ system with z-axis DM interaction, HF coupling distance, and in the presence of a uniform magnetic field. To the best of our knowledge, this study is the first to offer the first finding of thermal quantum correlation measured by negativity for two-spins-qudit over the HF coupling distance.

This paper is organized as follows: Section 2 presents in-depth the theoretical model of our system exposed to DM interaction and a magnetic field with HF coupling. In addition, we establish the spectrum of the system at a certain temperature. Section 3 will address thermal quantum entanglement measured by negativity. Section 4 will include numerical studies to highlight the behavior of systems. Lastly, the investigation is concluded with a summary of the results.

2 Hamiltonian of the system

In this study, we take into account a Heisenberg XXZ model with two-qudit (spin 1), Herring-Flicker (HF) coupling, and z-axis DM interaction exposed to a uniform magnetic field. The Hamiltonian of the system is expressed by

$$\mathcal{H} = \mathcal{H}_H + \mathcal{H}_{DM} + \mathcal{H}_Z \quad (1)$$

\mathcal{H}_H corresponds to the XXZ Heisenberg chain, \mathcal{H}_{DM} indicates the DM interaction, and \mathcal{H}_Z refers to the Zeeman energy. Usually, the DM Hamiltonian \mathcal{H}_{DM} [47, 48] can be represented as follows

$$\begin{aligned} \mathcal{H}_{DM} &= \vec{D} \cdot (\vec{\sigma}_1 \times \vec{\sigma}_2) \\ &= D_x (\sigma_1^y \sigma_2^z - \sigma_1^z \sigma_2^y) + D_y (\sigma_1^x \sigma_2^z - \sigma_1^z \sigma_2^x) + D_z (\sigma_1^x \sigma_2^y - \sigma_1^y \sigma_2^x) \end{aligned} \quad (2)$$

Where $\sigma^{x,y,z}$ denotes the Pauli matrices for a spin-1 and $D_{x,y,z}$ reflects the components of DM interaction. In the current studies, we limit ourselves to the case where the DM interaction occurs along the z-axis. Then, our Hamiltonian has the form

$$\mathcal{H} = J (\sigma_1^x \sigma_2^x + \sigma_1^y \sigma_2^y + \gamma \sigma_1^z \sigma_2^z) + D_z (\sigma_1^x \sigma_2^y - \sigma_1^y \sigma_2^x) + B (\sigma_1^z + \sigma_2^z) \quad (3)$$

where $\sigma^m (m = x, y, z)$ denotes the spin-1 Pauli matrices given by

$$\sigma^x = \frac{1}{\sqrt{2}} \begin{pmatrix} 0 & 1 & 0 \\ 1 & 0 & 1 \\ 0 & 1 & 0 \end{pmatrix}, \quad \sigma^y = \frac{1}{\sqrt{2}} \begin{pmatrix} 0 & -i & 0 \\ i & 0 & -i \\ 0 & i & 0 \end{pmatrix}, \quad \sigma^z = \begin{pmatrix} 1 & 0 & 0 \\ 0 & 0 & 0 \\ 0 & 0 & -1 \end{pmatrix} \quad (4)$$

and D_z denotes the DM interaction along the z-axis. It should be noted that J represents the coupling between the spin chains. Whenever the value of $J > 0$, the chain is antiferromagnetic; whenever the value of $J < 0$, the chain is ferromagnetic; γ is the anisotropy parameter. Furthermore, we assume that the coupling J is an HF coupling, i.e., $J(R)$, is defined by

$$J(R) = 1.642 \exp(-2R) R^{\frac{5}{2}} + O(R^2 \exp(-2R)) \quad (5)$$

Where R is HF coupling distance. The graph of the function J in terms of R is shown in Figure 1. From Fig. 1, it is evident that the coupling of HF is zero when the spins are far apart

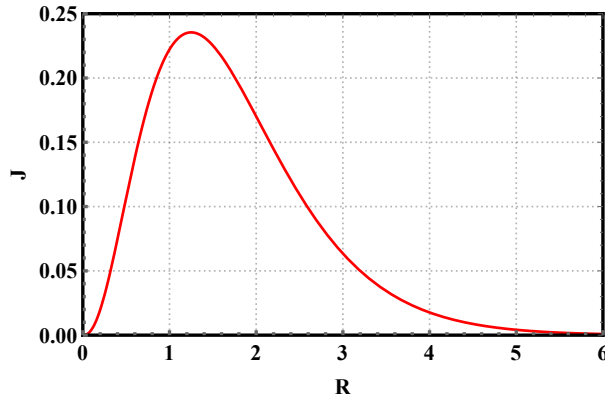


Figure 1 – (Color online) The coupling J of Herring-Flicker in terms of the distance R between two spins.

($R > 6$) and has a maximum when they are closer ($R \simeq 1.3$), implying that the spins become free at greater distances. As a result, in this study, we restrict ourselves to values on the margin where J is non-zero ($0 < R < 6$).

To evaluate the spectrum of the Hamiltonian (3) it is convenient to give the matrix form of \mathcal{H} in the basis $|-1, -1\rangle, |-1, 0\rangle, |-1, 1\rangle, |0, -1\rangle, |0, 0\rangle, |0, 1\rangle, |1, -1\rangle, |1, 0\rangle, |1, 1\rangle$ as

$$\mathcal{H} = \begin{pmatrix} \gamma J(R) + 2B & 0 & 0 & 0 & 0 & 0 & 0 & 0 & 0 \\ 0 & B & 0 & re^{i\theta} & 0 & 0 & 0 & 0 & 0 \\ 0 & 0 & -\gamma J(R) & 0 & re^{i\theta} & 0 & 0 & 0 & 0 \\ 0 & re^{-i\theta} & 0 & B & 0 & 0 & 0 & 0 & 0 \\ 0 & 0 & re^{-i\theta} & 0 & 0 & 0 & re^{i\theta} & 0 & 0 \\ 0 & 0 & 0 & 0 & 0 & -B & 0 & re^{i\theta} & 0 \\ 0 & 0 & 0 & 0 & re^{-i\theta} & 0 & -\gamma J(R) & 0 & 0 \\ 0 & 0 & 0 & 0 & 0 & re^{-i\theta} & 0 & -B & 0 \\ 0 & 0 & 0 & 0 & 0 & 0 & 0 & 0 & \gamma J(R) - 2B \end{pmatrix} \quad (6)$$

which the quantities r and θ are defined by

$$r = \sqrt{D_z^2 + J(R)^2} \quad (7)$$

$$\theta = \arctan\left(\frac{D_z}{J(R)}\right) \quad (8)$$

the eigenvalues as well as the eigenvectors of the equation (6) are given by

$$\epsilon_{1,2} = B \pm r \quad (9)$$

$$\epsilon_{3,4} = \gamma J(R) \pm 2B \quad (10)$$

$$\epsilon_5 = -\gamma J(R) \quad (11)$$

$$\epsilon_{6,7} = -B \pm r \quad (12)$$

$$\epsilon_{8,9} = \frac{r}{2} \chi_{2,1} \quad (13)$$

where $\chi_{1,2} = \frac{\sqrt{\gamma^2 J(R)^2 + 8r^2} \pm \gamma J(R)}{r}$, and the related eigenvectors

$$\begin{aligned}
|\varphi_{1,2}\rangle &= \pm \frac{e^{i\theta}}{\sqrt{2}} |-1, 0\rangle + \frac{1}{\sqrt{2}} |0, -1\rangle \\
|\varphi_{3,4}\rangle &= |\mp 1, \mp 1\rangle \\
|\varphi_5\rangle &= -\frac{e^{2i\theta}}{\sqrt{2}} |-1, 1\rangle + \frac{1}{\sqrt{2}} |1, -1\rangle \\
|\varphi_{6,7}\rangle &= \pm \frac{e^{i\theta}}{\sqrt{2}} |0, 1\rangle + \frac{1}{\sqrt{2}} |1, 0\rangle \\
|\varphi_{8,9}\rangle &= \frac{2e^{2i\theta}}{\sqrt{\chi_{1,2}^2 + 8}} |-1, 1\rangle \pm \frac{e^{i\theta}\chi_{1,2}}{\sqrt{\chi_{1,2}^2 + 8}} |0, 0\rangle + \frac{2}{\sqrt{\chi_{1,2}^2 + 8}} |1, -1\rangle
\end{aligned} \tag{14}$$

After obtaining the spectrum of our system, it is easy to calculate the thermal density, which is essential for performing measurements of the examined system's entanglement. To this end, the following section will be devoted to calculating the density matrix following the system's parameters.

3 Thermal density matrix and negativity

After determining the system's spectrum, we shall seek the equation of the density matrix $\varrho(T)$, which will enable us to quantify the negativity at the thermal thermodynamic equilibrium at a given temperature T . According to the above-described framework, the system's state of thermal equilibrium might be expressed as follows

$$\varrho(T) = \frac{1}{\mathbb{Z}} e^{-\beta\mathcal{H}} \tag{15}$$

such that the canonical partition function \mathbb{Z} is written by

$$\mathbb{Z} = \sum_{i=1}^9 e^{-\beta\epsilon_i} \tag{16}$$

such as k_B is the constant of the Boltzmann, for convenience, it is considered as unity in the next. The temperature's inverse is represented by the parameter $\beta = 1/T$. The spectrum of the Hamiltonian (6) allows expressing the thermal density $\varrho(T)$ as

$$\varrho(T) = \frac{1}{\mathbb{Z}} \sum_{k=1}^4 e^{-\beta\epsilon_k} |\phi_k\rangle\langle\phi_k| \tag{17}$$

Adding equations (9) and (14) to equation (17) yields the density matrix of the system in thermal equilibrium, which may be written on the previous basis as

$$\varrho(T) = \frac{1}{\mathbb{Z}} \begin{pmatrix} \rho_{11} & 0 & 0 & 0 & 0 & 0 & 0 & 0 & 0 \\ 0 & \rho_{22} & 0 & e^{i\theta}\rho_{24} & 0 & 0 & 0 & 0 & 0 \\ 0 & 0 & \rho_{33} & 0 & e^{i\theta}\rho_{35} & 0 & e^{2i\theta}\rho_{37} & 0 & 0 \\ 0 & e^{-i\theta}\rho_{42} & 0 & \rho_{44} & 0 & 0 & 0 & 0 & 0 \\ 0 & 0 & e^{-i\theta}\rho_{53} & 0 & \rho_{55} & 0 & e^{i\theta}\rho_{57} & 0 & 0 \\ 0 & 0 & 0 & 0 & 0 & \rho_{66} & 0 & e^{i\theta}\rho_{68} & 0 \\ 0 & 0 & e^{-2i\theta}\rho_{73} & 0 & e^{-i\theta}\rho_{75} & 0 & \rho_{77} & 0 & 0 \\ 0 & 0 & 0 & 0 & 0 & e^{-i\theta}\rho_{86} & 0 & \rho_{88} & 0 \\ 0 & 0 & 0 & 0 & 0 & 0 & 0 & 0 & \rho_{99} \end{pmatrix} \tag{18}$$

such that the density matrix elements are given by

$$\begin{aligned}
\varrho_{11} &= e^{-\beta(2B+\gamma J(R))} \\
\varrho_{22} &= \varrho_{44} = e^{-\beta B} \cosh(\beta r) \\
\varrho_{33} &= \varrho_{77} = \frac{1}{2} e^{\beta \gamma J(R)} + \frac{4e^{-\frac{\beta r \chi_2}{2}}}{\chi_1^2 + 8} + \frac{4e^{\frac{\beta r \chi_1}{2}}}{\chi_2^2 + 8} \\
\varrho_{55} &= \frac{\chi_1^2 e^{-\frac{1}{2} \beta r \chi_2}}{\chi_1^2 + 8} + \frac{\chi_2^2 e^{\frac{1}{2} \beta r \chi_1}}{\chi_2^2 + 8} \\
\varrho_{37} &= \varrho_{73} = \frac{1}{2} \left(-e^{\beta \gamma J(R)} + \frac{8e^{-\frac{\beta r \chi_2}{2}}}{\chi_1^2 + 8} + \frac{8e^{\frac{\beta r \chi_1}{2}}}{\chi_2^2 + 8} \right) \\
\varrho_{35} &= \varrho_{53} = \varrho_{57} = \varrho_{75} = -\frac{4 \left(e^{\frac{\beta \gamma J(R)}{2}} \sinh \left(\frac{1}{4} \beta r (\chi_1 + \chi_2) \right) \right)}{\chi_1 + \chi_2} \\
\varrho_{66} &= \varrho_{88} = e^{\beta B} \cosh(\beta r) \\
\varrho_{24} &= \varrho_{42} = -e^{-\beta B} \sinh(\beta r) \\
\varrho_{68} &= \varrho_{86} = -e^{\beta B} \sinh(\beta r) \\
\varrho_{99} &= e^{\beta(2B-\gamma J)}
\end{aligned} \tag{19}$$

The negativity, based on the partial transposition approach [14], is shown to be a beneficial entanglement measurement introduced by Vidal et al. [37], and that it can be determined effectively for any dimension bipartite system. We shall use the method [49], as described by

$$\mathcal{N}(\varrho) = \sum_j |\lambda_j| \tag{20}$$

Where the negative eigenvalues of the partial transposition $\varrho^{T_1}(\varrho^{T_2})$ of the given state ϱ with consideration to the first (second) system are denoted by λ_j , in this case, the expression of ϱ^{T_1} is defined by

$$\varrho^{T_1} = \frac{1}{\mathbb{Z}} \begin{pmatrix} \varrho_{11} & 0 & 0 & 0 & e^{i\theta} \varrho_{24} & 0 & 0 & 0 & e^{2i\theta} \varrho_{37} \\ 0 & \varrho_{22} & 0 & 0 & 0 & e^{i\theta} \varrho_{35} & 0 & 0 & 0 \\ 0 & 0 & \varrho_{33} & 0 & 0 & 0 & 0 & 0 & 0 \\ 0 & 0 & 0 & \varrho_{44} & 0 & 0 & 0 & e^{i\theta} \varrho_{57} & 0 \\ e^{-i\theta} \varrho_{42} & 0 & 0 & 0 & \varrho_{55} & 0 & 0 & 0 & e^{i\theta} \varrho_{68} \\ 0 & e^{-i\theta} \varrho_{53} & 0 & 0 & 0 & \varrho_{66} & 0 & 0 & 0 \\ 0 & 0 & 0 & 0 & 0 & 0 & \varrho_{77} & 0 & 0 \\ 0 & 0 & 0 & e^{-i\theta} \varrho_{75} & 0 & 0 & 0 & \varrho_{88} & 0 \\ e^{-2i\theta} \varrho_{73} & 0 & 0 & 0 & e^{-i\theta} \varrho_{86} & 0 & 0 & 0 & \varrho_{99} \end{pmatrix}. \tag{21}$$

We currently have all we need to investigate the behavior of our system. To do this, we will devote the following part to a numerical analysis of the negativity \mathcal{N} , as detailed below, to demonstrate the full performance of the proposed system. Then, we presented some graphs depending on the parameters of the system under consideration, like temperature T , HF coupling distance R , DM interaction D_z and uniform magnetic field B . In addition, we will continue to examine this in more detail in order to draw conclusions.

4 Numerical results

This section will quantitatively investigate several elements of entanglement in a two–spin–qudit Heisenberg XXZ chain with z –axis of DM interaction in terms of the HF coupling distance R for various temperatures and magnetic field values. Firstly, we will explore negativity \mathcal{N} as a function of temperature T for different R and magnetic field values by fixing the z –axis DM interaction such as $D_z = 1$. Secondly, for a given temperature T , coupling distance R , and magnetic field B , we display the negativity \mathcal{N} as a function of z –axis DM interaction. Finally, we will adjust the z –axis DM interaction for the value $D_z = 1$ to plot the negativity \mathcal{N} as a function of the HF coupling distance R , temperature T , and magnetic field B .

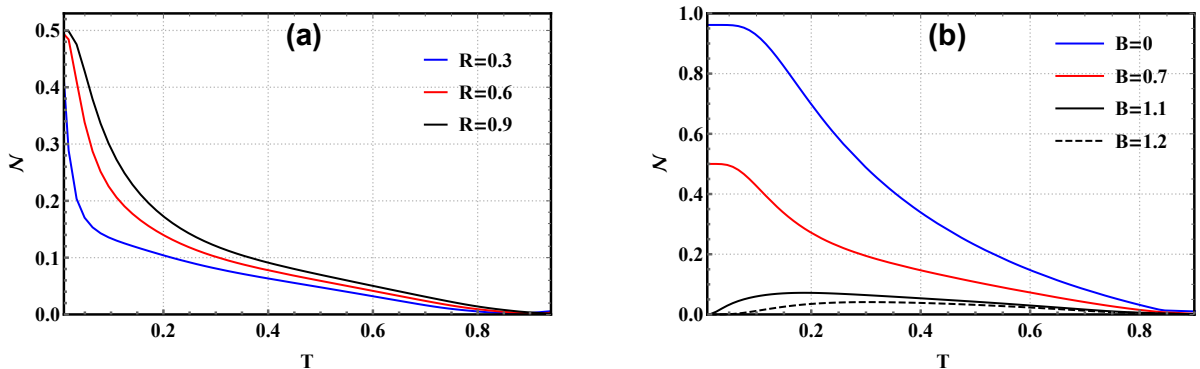


Figure 2 – (Color online) (a) The negativity versus T for different R for $B = D_z = 1$. (b) The negativity versus T for different B for the values $D_z = 1$ and $R = 0.5$.

In figure (2), we plot the negativity \mathcal{N} as a function of temperature for different HF coupling distances R (Fig. 2(a)) and magnetic field B (Fig. 2(b)). In Fig. 2(a), the negativity is plotted as a function of the temperature T for $R = 0.3, 0.6, 0.9$ and the other parameters are set as $D_z = B = 1$. At high temperatures, the negativity is cancelled, which means that the state’s system becomes separable. Moreover, for a fixed value of T , the negativity increases with increasing HF coupling distance R . From Fig. 2(b) when $B = 0$, the maximally entangled state $|\varphi_2\rangle = |\varphi_7\rangle$ is the ground state with eigenvalue $-r$ with the maximum entanglement, i.e., $N = 0.9616$. Furthermore, when T rises, the negativity lowers owing to the mixture of other states with the maximally entangled state. The state $|11\rangle$ is changing into the ground state for strong magnetic fields B ($B = 1.2$), meaning that there is no entanglement at $T = 0$. As a result, as T grows, the maximally entangled states mix with the unentangled state $|11\rangle$, hence increasing entanglement. Negativity decreases with rising magnetic field B for a given value of T until it reaches zero at higher temperatures.

Figure 3 shows the entanglement change with D_z in the two–particle antiferromagnetic XXZ model ($J > 0$) with different parameters (T , R and B). The first remark is that the negativity is symmetrical compared to $D_z = 0$. For this, we will interpret only the positive values of D_z . The negativity remains null for a certain value of D_z lower than the critical value D_z^c , this last varying according to the parameters T , R or B . However, the rise of the quantities T and R decreases the critical value of D_z^c (Figs. 3(a) and (b)). On the other hand, when the magnetic field increases, the D_z^c critical value increases (Fig. 3(c)). In addition, we observe a peak of

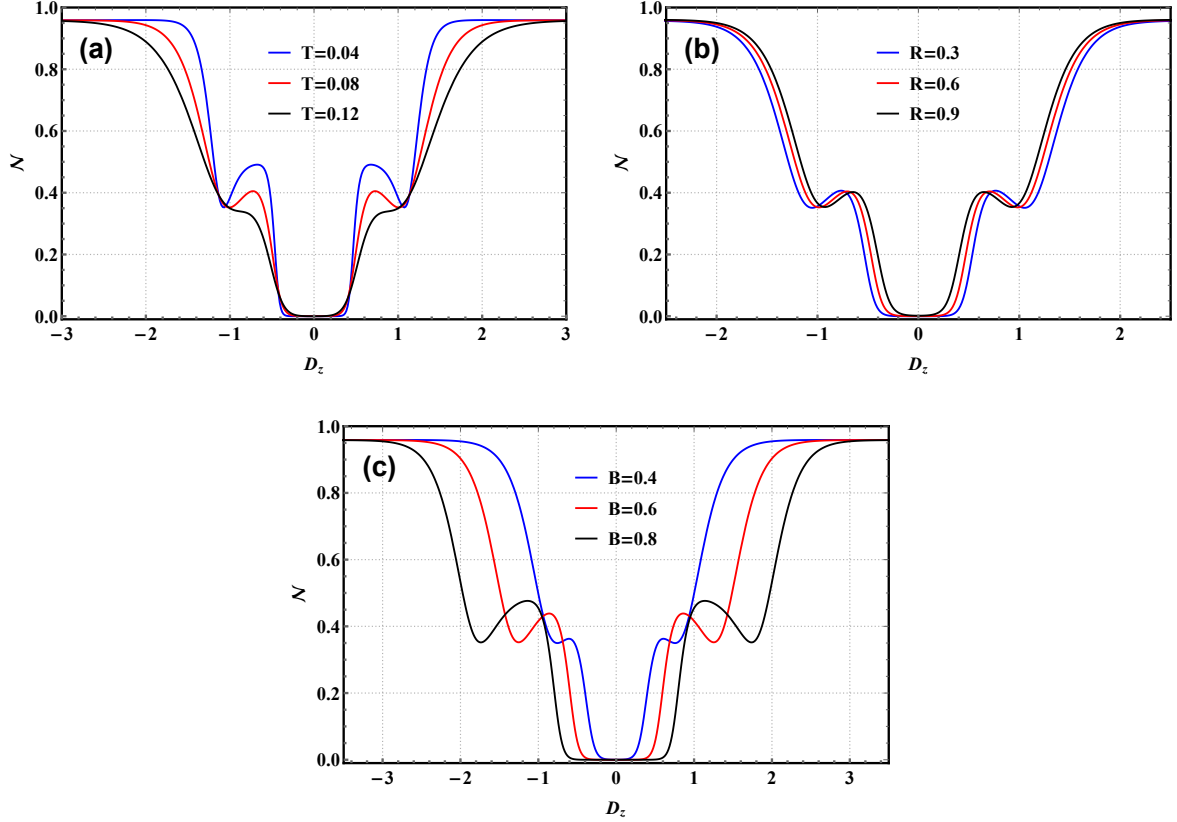


Figure 3 – (Color online) The negativity versus z -axis DM interaction. (a) for different T ($R = B = 1$), (b) for different R ($T = 0.08$ and $B = 0.5$), (c) for different B ($T = 0.08$ and $R = 0.5$).

negativity which is related to the temperature T , HF coupling distance R and magnetic field B . Indeed, for $D_z > D_z^c$ and in the vicinity of $D_z = 1$, the negativity presents a peak that vanishes with the temperature increase. Physically, the disappearing of the peak can be explained by the temperature dominance in the DM interaction, which is shown in Fig. 3(a). In Fig. 3(b) and for the interval $D_z^c < D_z < 1$, we find the same behavior as in Fig. 3(a), except that the HF coupling is significant in this interval. Moreover, in Fig. 3(c), the peaks always appear with increasing amplitudes as the magnetic field increases. Finally, when the DM interaction parameter D_z is very high, the negativity of the entanglement approaches an identical maximum fixed value in all three figures, which means that the state's system is maximally entangled.

In Fig. 4, we display the negativity \mathcal{N} as a function of the HF coupling distance parameter R (Fig. 4(a)), the uniform magnetic field B (Fig. 4(b)) at different temperature values (0.04, 0.08, 0.12 and 0.5) and the uniform magnetic field B at $T = 0$ (Fig. 4(c)). In Fig. 4(a), we see that the negativity \mathcal{N} increases when the parameter R increases in the XXZ system with DM interaction ($D_z = 1$) and in the presence of a magnetic field ($B = 1$). When the HF coupling distance parameter R is large, the negativity tends to be constant even as the temperature rises. Furthermore, it is clear that as the temperature rises, the entanglement vanishes even if R varied, which is explained by the dominance of the temperature (black dashed curve). From Figures 4(b) and 4(c), we see that there is evidence of phase transition at low temperature by increasing the magnetic field B . When B is small, the entanglement is initially at its maximum. When the uniform magnetic field B is greater, the entanglement decreases until it takes on a

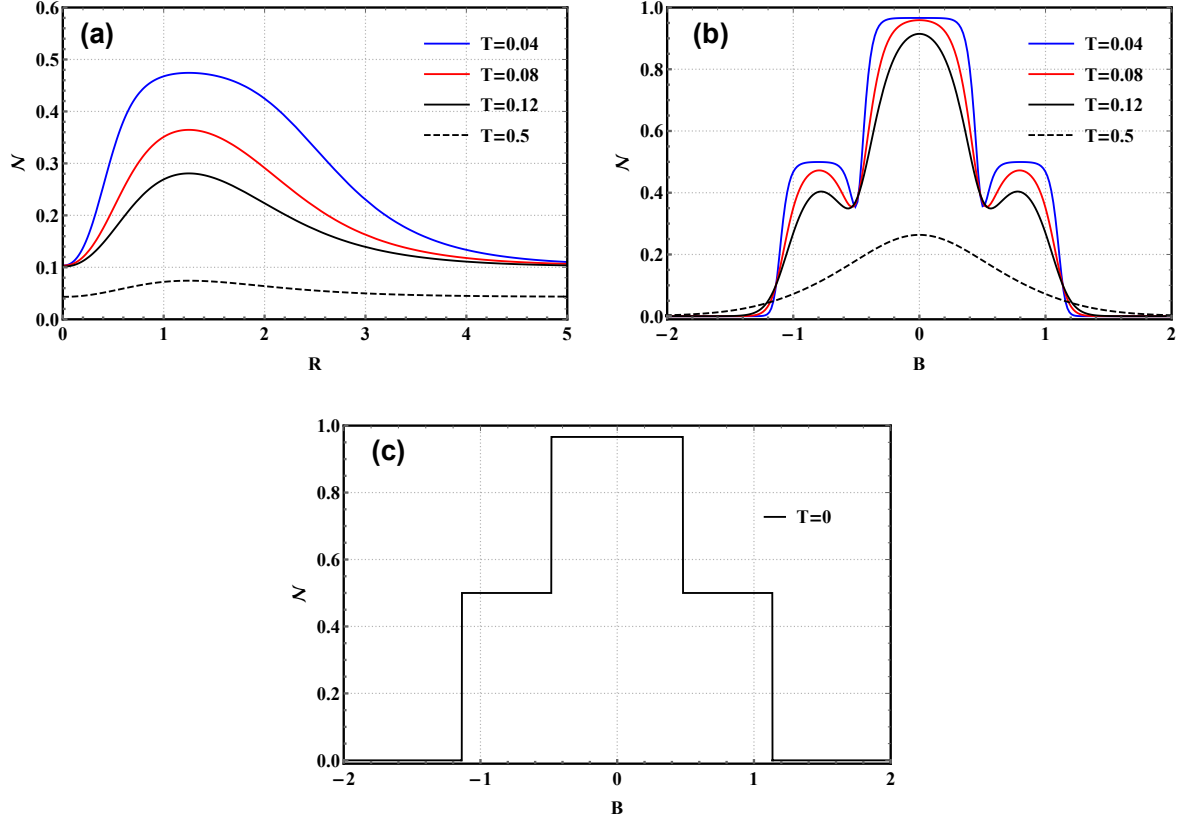


Figure 4 – (Color online) (a): The negativity in terms of R ($B = D_z = 1$), and (b,c): versus B ($R = D_z = 1$) for different value of T .

null value. At $T = 0$, we can also see that the entanglement vanishes when B crosses a critical point B_c . However, the role of magnetic fields is mainly to reduce entanglement.

5 summary

In this paper, we have explored thermal quantum entanglements by using the negativity concept to discuss the entanglement of a two-qutrit Heisenberg XXZ chain subjected to the uniform magnetic field and z -axis DM interaction with the distance of the HF coupling. The Hamiltonian model is described, the spectrum entanglement has been determined through mathematical calculations, and the thermal state at a finite temperature is mentioned explicitly. The numerical behavior of the negativity-measured entanglements in our study has been examined in terms of temperature, z -axis DM interaction, HF distance coupling and uniform magnetic field. The ground state entanglement at zero temperature has been analyzed. We discovered that negativity declines monotonically with increasing temperature, and it is also clear that the magnetic field eliminates entanglement. Furthermore, We have also looked into the z -axis DM interaction parameter D_z , which can be raised to enhance entanglement. Finally, the affect of the HF coupling distance R on quantum entanglement in spin systems is explored, i.e., decreasing the temperature can improve the entanglement of the system states.

References

- [1] A. Einstein, B. Podolsky, and N. Rosen, *Phys. Rev.* **47** (1935) 777
- [2] R. Houça, A. Belouad, E. B. Choubabi, A. Kamal, and M. El Bouziani, *J. Magn. Magn. Mater.* **563** (2022) 169816
- [3] C. H. Bennett, F. Brassard, C. Crepear, and al, *Phys. Rev. Lett.* **70** (1993) 1895
- [4] A. K. Ekert, *Phys. Rev. Lett.* **67** (1991) 661
- [5] D. P. Divincenzo, D. Eacon, J. Kempe, and al, *Nat.* **408** (2000) 339
- [6] L. K. Grover, *Phys. Rev. Lett.* **79** (1997) 4709
- [7] P. W. Shor, *I. Found. o. Comp. Sci.* **35** (1994) 124
- [8] S. Khan, M. Ramzan, and M. K. Khan, *Chin. Phys. Lett.* **27** (2010) 080302
- [9] J. Brendel, N. Gisin, W. Tittel, and H. Zbinden, *Phys. Rev. Lett.* **82** (1999) 2594
- [10] D. Kielpinski, C. Monroe, and D. J. Wineland, *Nat.* **417** (2002) 709
- [11] L. Bogani, and W. Wernsdorfer, *A Collec. of Rev. from Nat. Jour.* (2010) 194
- [12] N. M. Chtchelkatchev, G. Blatter, G. B. Lesovik, and T. Martin, *Phys. Rev. B.* **66** (2002) 161320
- [13] R. Folman, P. Krüger, D. Cassettari, B. Hessmo, T. Maier, and J. Schmied-mayer, *Phys. Rev. Lett.* **84** (2000) 4749
- [14] A. Peres, *Phys. Lett.* **77** (1996) 1413
- [15] M. Horodecki, P. Horodecki, and R. Horodecki, *Phys. Lett. A.* **1** (1996) 223
- [16] K. Zyczkowski, P. Horodecki, A. Sanpera, and M. Lewenstein, *Phys. Rev. A.* **58** (1998) 883
- [17] G. Vidal, and R. F. Werner, *Phys. Rev. A.* **65** (2002) 032314
- [18] M. C. Amesen, S. Bose, and V. Vedral, *Phys. Rev. Lett.* **87** (2001) 017901
- [19] X. G. Wang, *Phys. Rev. A* **64** (2001) 012313
- [20] L. Zhou, H. S. Song, Y. Q. Guo, and C. Li, *Phys. Rev. A.* **68** (2003) 024301
- [21] G. F. Zhang, and S. S. Li, *Phys. Rev. A.* **72** (2005) 034302
- [22] J. L. Guo, and H. S. Song, *Eur. Phys. J. D.* **56** (2010) 265
- [23] T. Tufarelli, D. Girolami, R. Vasile, S. Bose, and G. Adesso, *Phys. Rev. A.* **S86** (2012) 052326
- [24] Y. Yao, and al, *Phys. Rev. A.* **86** (2012) 062310
- [25] S. Xu, X. K. Song, and L. Ye, *Int. J. Mod. Phys. B.* **27** (2013) 1350074

- [26] Y. Yao, and al. Phys. Rev. A. **86** (2012) 042102
- [27] F. W. Ma, S. X. Liu, and X. M. Kong, Phys. Rev. A. **84** (2011) 042302
- [28] X. G. Wang, Phys. Rev. A. **64** (2001) 012313
- [29] X. G. Wang, Phys. Rev. A. **66** (2002) 034302
- [30] R. Houça, A. Belouad, E. B. Choubabi, A. Kamal, and M. El Bouziani, Quant. Infor. Proc. **21** (2022) 1
- [31] M. A. Nielsen, "Quantum information theory" PhD thesis, University of New Mexico (1998).
arXiv:quant-ph/0011036
- [32] M. C. Arnesen, S. Bose, and V. Vedral, Phys. Rev. Lett. **87** (2001) 017901
- [33] G. L. Kamta, and A F. Starace, Phys. Rev. Lett. **88** (2002) 107901
- [34] X. G. Wang, Phys. Lett. A. **281** (2001) 101
- [35] L. Zhou, H. S. Song, Y. Q. Guo, et al. Phys. Rev. A. **68** (2003) 024301
- [36] K. W. William, Phys. Rev. Lett. **80** (1998) 2245
- [37] G. Vidal, R. F. Phys. Rev. A. **65** (2002) 032314
- [38] J. Schliemann, Phys. Rev. A. **68** (2003) 012309
- [39] G. F. Zhang, and S S. Li, S. S. Comm. **138** (2006) 17
- [40] G. F. Zhang, Eur. Phys. J. D. **37** (2006) 123
- [41] Z. Sun, X. Wang , and Y. Q. Li, N. J. Phys. **7** (2005) 83
- [42] X. Wang, H. B. Li, Z. Sun, et al, J. Phys. A. **38** (2005) 870
- [43] F. D. M. Haldane, Phys. Rev. Lett., **60**, (1988) 635.
- [44] B. S. Shastry, Phys. Rev. Lett., **60**, (1988) 639.
- [45] B. Lin, Y. S. Wang , Physica B. **407**, (2012) 77
- [46] M. XiaoSan, Q. Ying, Z. GuangXing and W. AnMin, Science China, **56**, (2013) 600
- [47] T. Moriya, Phys. Rev. **120** (1960) 91
- [48] T. Moriya, Phys. Rev. Lett. **4** (1960) 228
- [49] A. Miranowicz, and A. Grudka, J. Opt. B. Quant. Semiclass. Opt. **6** (2004) 542